Applied Scientific Research **52:** 21–35, 1994.

Macrosegregation in Continuously Cast Steel Billets and Blooms

R.J.A. JANSSEN and G.C.J. BART
Department of Applied Physics, Delft University of Technology, P.O. Box 5046, 2600 GA Delft, The Netherlands

and

M.C.M. CORNELISSEN and J.M. RABENBERG
Hoogovens Research and Development Laboratories, P.O. Box 10000, 1970 CA IJmuiden, The Netherlands

(Received: 5 February 1992; accepted in revised form: 8 June 1992)

Abstract. In this paper, a study of the centerline macrosegregation phenomenon which occurs often in the industrial casting of steel billets is described. Previous work on this subject was reviewed and it was concluded that the most likely explanation of this macrosegregation, is the occurrence of *internal* deformations in the solid, dendrite skeleton of the solidifying steel. After modelling these deformations, a simplified computational procedure to solve the transport and deformation equations describing the solidification process was devised. Care has been taken to ensure that the entire computational procedure can be implemented within a Computational Fluid Dynamics code, PHOENICS. The results of preliminary computations show good agreement between calculations and experiments and hence show that internal deformations in solidifying blooms and billets are the main cause of centerline macrosegregation.

1. Introduction

Over the past 25 years, a lot of attention has been paid to studies of the solidification process of metal alloys. Attention has been focused on the solidification in industrial casting processes and has mainly concerned either aluminum or steel alloys, because of their huge industrial and economic importance.

One of the most intrigueing problems the industry faces with respect to casting processes, is the fact that usually, the chemical composition of the steel is not uniform. In the steel industry this problem has plagued manufacturers both with the old, static, ingot casting process as well as with the more recent continuous casting process.

Two kinds of segregation can be observed: one, the so called microsegregation demonstrates itself at the length scale of the dendrites (typically 10–100 μm); the other, called macrosegregation, occurs at the length scale of the cast product itself. Both types of segregation have the same *principal* cause: the difference between the solubility of the dissolved elements in the liquid phase and in the solid phase.

The problems in industry are caused by the macrosegregation effect. Since segregation effects can be large (the concentration of the elements dissolved in the

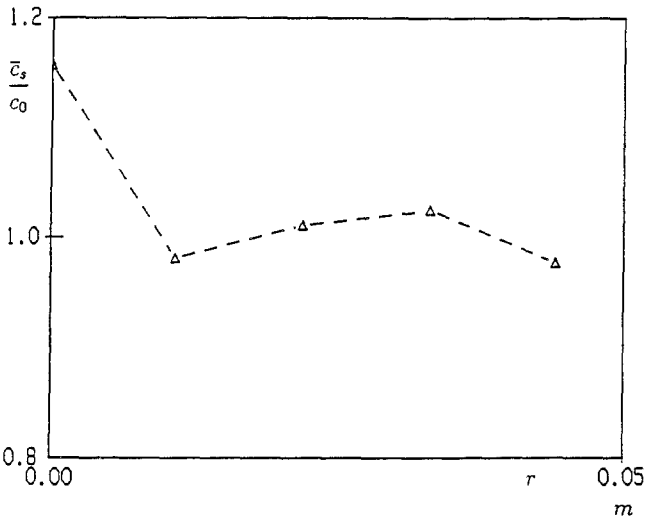

Fig. 1. Measured concentration distribution of carbon as a function of the distance to the surface of the cast product.

steel, can vary as much as a quarter of their nominal values), macrosegregation puts limits on the castability of specific steel grades. It would therefore obviously be of great economic importance if it were possible to control the solidification process in such a way as to counter the macrosegregation. This can be done by using electromagnetic stirrers to enhance mixing of the liquid steel in the solidifying product. Another way would be to change the cooling conditions, under which the solidification takes place, in such a way that a uniform composition is obtained. Before using such methods in practice, it would be helpfull if numerical simulations could be performed to predict the influence of these actions on the formation of macrosegregation.

Our research was aimed at finding a theory to explain the cause of macrosegregation and, more specifically, to explain and calculate one particular kind of macrosegregation: the *centerline* macrosegregation. An example of this kind of segregation, typical for high carbon steel grades, is given in Figure 1 (obtained from measurements performed at the Hoogovens Steelworks in The Netherlands). The two characteristic features of the distribution shown in Figure 1 are the peak of positive segregation in the center of the cast product and the minimum corresponding to negative segregation just near the peak.

The solidification of steel in a casting machine is a complex process involving the transport of heat, liquid steel and the elements dissolved in the steel. These transport processes are described by differential equations expressing mathematically the conservation of mass, solute mass, heat and liquid steel momentum. Hence, to calculate the segregation these equations have to be solved. Since all these equations show the same mathematical structure, a commercial software code known as PHOENICS [13] could be used to solve them, reducing the time spent

on programming. PHOENICS is a general Computational Fluid Dynamics code, specially written to solve transport equations of the kind encountered in this study.

This study closely follows the work by Lesoult *et al.* presented in [8, 9, 10]. However, whereas in these references a Lagrangian formulation is used to express the governing equations, the more common Eulerian formulation has been used in this study which made it possible for us to use the PHOENICS code. Also, the computational procedure, as explained in section 5 of this article, differs from the one proposed in [8, 9, 10].

2. Formation of Macrosegregation

Several mechanisms have been proposed to explain the observed macrosegregation:

1. Interdendritic flow of liquid steel due to solidification shrinkage and changes in the density of the liquid. These density changes can be caused by temperature changes (natural convection) or by changes in the composition of the liquid steel ([6, 7, 11]).
2. Movements of both liquid and solid phases due to deformations of the dendritic layer in the mushy zone and of the solid shell ([8, 9, 10, 12]).
3. Diffusion of the dissolved elements in the liquid pool ([15]).

The actual calculation of macrosegregation (both numerical and in certain simplified situations, analytical), started with the publication by Flemings and his coworkers of their papers [6, 11] at the end of the sixties. Flemings derived a simple mathematical formulation, in which it was assumed that there was no transport or deformation of the solid. He also neglected diffusion within the liquid. Hence, he only considered fluid flow and assumed that this flow was caused by solidification shrinkage and by the dependence of the liquid density on temperature and composition (for the latter see also [7]). Flemings found a negative centerline segregation instead of the positive one usually observed. More importantly, the calculated segregation was an order of magnitude smaller than the experimentally observed one. Flemings performed some calculations for static ingots, but similar calculations were carried out in [14] for the continuous casting process with similar results. Hence, the conclusion was drawn that solidification shrinkage and density changes in the liquid are not an important cause of centerline macrosegregation.

Since the time these results were obtained, focus has shifted to other possible causes of macrosegregation, of which deformations of the solid shell and of the solid, dendritic skeleton in the mushy zone, have received most attention. In this respect the study in [12] by Miyazawa certainly has to be mentioned, in which macrosegregation in continuously cast steel slabs was calculated. In this study, deformations were caused by bulging of the slab between the rolls which support it during casting i.e., only *externally* prescribed deformations were assumed. *Internal* deformations were not taken into account. Miyazawa's study was the first one

to actually achieve a good agreement between numerical results and practical evidence.

However, in the case of continuously cast steel billets and blooms, there are only a few supporting rolls and it is therefore unlikely that external deformations of the type Miyazawa assumed, are the cause of segregation. Recently, Lesoult *et al.* have presented in [8, 9, 10] results of calculations in which internal deformations of the dendritic layer, caused by thermal contractions and expansions, are considered to be the main cause of macrosegregation. Again, a good agreement between numerical results and practical evidence was obtained.

Hence, in this study, emphasis is placed on *internal* deformations of the solid phase as the main cause of macrosegregation.

3. Governing Equations

The solidification of steel in a casting machine is a complex process involving a mixture of liquid and solid iron in which severable elements are dissolved. The most difficult part of the steel to describe is the mushy zone in which a complex structure of dendrites is formed between which there is a flow of interdendritic fluid. Due to the different solubilities of the dissolved elements in solid and liquid iron, this interdendritic fluid is rich in solute elements. Hence, displacement of this fluid can cause segregation effects. As stated in the previous section, we assume that deformations (more in particular internal deformations) are the main cause of macrosegregation. To actually calculate this macrosegregation, several transport equations describing mathematically the conservation of mass, solute mass, energy and liquid steel momentum, have to be solved.

In this section the transport equations for the continuous casting process will be presented. The objective here is to present the equations in the form in which they were used in the numerical study. A full and extensive mathematical derivation of the equations will not be presented as the equations are all (except for the equation expressing the conservation of solute mass) in a 'standard' form, common for two-phase flows (see for instance [1]). The assumptions made when these equations were derived, are the following:

1. Only the steady state is considered.
2. There are no microscopic concentration gradients in the interdendritic liquid, due to the high diffusivity of solute in the liquid and the small dendrite arm spacing.
3. The ratio between the concentration of solute i in the solid at the microscopic solid/liquid interface, c_{si}^*, and the concentration in the liquid, c_{li}, is given by the equilibrium distribution ration k_i.
4. Diffusion in the solid is neglected (on a *macroscopic* scale that is). This hypothesis is supported by the result of the work in [15], in which a numerical study to calculate the influence of diffusion was performed.

Hence, the interest is in equations describing the steady state casting process, in which convective transport and thermal conduction are taken into consideration and deformations of the solid phase are allowed for.

Mass balance
We consider an element of volume located in the flowing steel string of the continuous casting process. This volume element is located at a fixed position relative to the casting machine and the steel moves through it. An equation that accounts for the conservation of mass over the volume element is given by

$$\nabla \cdot (\rho_l f_l \vec{v}_l + \rho_s f_s \vec{v}_s) = 0, \tag{1}$$

where ρ, f and $\vec{v}$ denote density, volume fraction and velocity respectively and where the subscripts l and s denote the liquid and the solid phase respectively.

The two terms $\nabla \cdot (\rho_l f_l \vec{v}_l)$ and $\nabla \cdot (\rho_s f_s \vec{v}_s)$ can be interpreted as the net mass flow of the liquid phase and the solid phase respectively, out of the volume element under consideration. Since only the steady state is considered, there is no mass change in the volume element and therefore both terms sum to zero.

Implicit in using Equation (1) is the assumption that the volume element is large enough to ensure that the definition of a volume fraction makes sense, but small enough that it can be treated as a differential element.

Solute mass balance
The solute mass balance is given by a corresponding equation:

$$\nabla \cdot (\rho_l f_l \vec{v}_l c_{li} + \rho_s f_s \vec{v}_s \bar{c}_{si}) = 0. \tag{2}$$

In Equation (2), $\bar{c}_{si}$ represents the *average* concentration of solute i in the solid phase of the volume element. Since it has been assumed that this volume element is large enough to ensure a sensible definition of a volume fraction, one has to distinguish between the *average* concentration of solute i in the solid phase, $\bar{c}_{si}$, in the volume element and the concentration in the solid c^*_{si} at the microscopic solid/liquid *interface*. This is so, because diffusion in the solid is usually small (the exception being carbon). In contrast to this, it can usually be safely assumed that diffusion in the liquid is large enough to ensure that c_{li} is uniform within the volume element (assumption (2) at the beginning of this section).

Since equation (2) expresses the conservation of solute mass in an element of volume, the concentration of solute i can be calculated from it. However, this leads to the problem that in equation (2) there are two unknown concentrations: c_{li} and $\bar{c}_{si}$. This means that an additional equation, linking c_{li} and $\bar{c}_{si}$ with each other, is needed. This additional equation can be found by considering microsegregation and by recalling the fact that $\nabla \cdot (\rho_s f_s \vec{v}_s \bar{c}_{si})$ is the mass of solute i, solidifying in the volume element, per time unit and per volume unit.

As far as microsegregation is concerned, one can distinguish between two limiting cases: in the first case there is no diffusion in the solid. This means that the

mass of solute i solidifying will be equal to the mass of solute i with concentration c^*_{si} in the envelope with total mass $\nabla \cdot (\rho_s f_s \vec{v}_s)$ just solidified. Hence:

$$\nabla \cdot (\rho_s f_s \vec{v}_s \bar{c}_{si}) - c^*_{si} \nabla \cdot (\rho_s f_s \vec{v}_s).$$

Because of assumption 3, $c^*_{si} = k_i c_{li}$ can be written and it follows that:

$$\nabla \cdot (\rho_s f_s \vec{v}_s \bar{c}_{si}) = k_i c_{li} \nabla \cdot (\rho_s f_s \vec{v}_s). \tag{3}$$

In the second case, diffusion in the solid is complete and hence $\bar{c}_{si} = c^*_{si} = k_i c_{li}$ must hold. Substituting this expression in Equation (2) gives:

$$\nabla \cdot (\rho_s f_s \vec{v}_s \bar{c}_{si}) = k_i c_{li} \nabla \cdot (\rho_s f_s \vec{v}_s) + \rho_s f_s \vec{v}_s \cdot \vec{\nabla}(k_i c_{li}). \tag{4}$$

Equations 3 and 4 can be combined using a parameter γ_i:

$$\nabla \cdot (\rho_s f_s \vec{v}_s \bar{c}_{si}) = k_i c_{li} \nabla \cdot (\rho_s f_s \vec{v}_s) + \gamma_i \rho_s f_s \vec{v}_s \cdot \vec{\nabla}(k_i c_{li}). \tag{5}$$

The parameter γ_i varies between 0 and 1.* $\gamma_i = 0$ results in Equation (3), which describes the situation of no diffusion in the solid phase and $\gamma_i = 1$ results in Equation (4), in which there is complete diffusion in the solid. Intermediate cases can be thought of with some but not complete diffusion giving a value for γ_i between 0 and 1.

Equation 5 has to be rewritten because of the fact that implementing the second term on the righthand side within the PHOENICS code would give problems. This has to do with the fact that this term contains the scalar product of a velocity $\vec{v}_s$ and a gradient vector, which means that this term cannot be integrated in a conservative way over a control volume, as is the prescribed way within PHOENICS. Hence, Equation (5) is rewritten in the form:

$$\nabla \cdot (\rho_s f_s \vec{v}_s \bar{c}_{si}) = (1 - \gamma_i) k_i c_{li} \nabla \cdot (\rho_s f_s \vec{v}_s) + \gamma_i \nabla \cdot (\rho_s f_s k_i \vec{v}_s c_{li}).$$

Substitution of this equation in Equation (2) gives:

$$\nabla \cdot (\rho_l f_l \vec{v}_l c_{li}) = (\gamma_i - 1) k_i c_{li} \nabla \cdot (\rho_s f_s \vec{v}_s) - \gamma_i \nabla \cdot (\rho_s f_s k_i \vec{v}_s c_{li}). \tag{6}$$

Equation (6) is in the form suitable for implementation in PHOENICS.

Energy balance

The energy equation is given by:

$$\nabla \cdot (\rho_l f_l \vec{v}_l (c_{pl} T + L) + \rho_s f_s \vec{v}_s c_{ps} T) = \nabla \cdot (\lambda \vec{\nabla} T) \tag{7}$$

where c_p denotes the specific heat capacity, L the latent heat, T the temperature and λ the thermal conductivity. In the transition range, in which solid and liquid phases coexist, c_{pl} and c_{ps} are taken to be equal. Equation 7 expresses the balance between

* In the appendix we will describe a way to estimate this parameter by relating it to quantities in a microsegregation model.

on the one hand energy (both latent heat as well as sensible heat) convected out of the volume element and on the other hand the energy conducted into the element.

Momentum balance
Finally, the equation for the flow in the mushy zone is given by the well known d'Arcy-equation:

$$\vec{v}_l - \vec{v}_s = -\frac{K}{\mu f_l}(\vec{\nabla} p - \rho_l \vec{g}), \tag{8}$$

where K denotes permeability, p pressure, μ viscosity and $\vec{g}$ the gravitational acceleration. The d'Arcy-equation is a simplified form of the more general equations describing the conservation of momentum in two-phase flows (see for instance [1]). The d'Arcy-equation in fact gives the fluid velocity, $\vec{v}_l$, in a porous medium in which there are only two external forces working on the fluid: the gravitational force and the friction exerted by the solid phase on the fluid. A measure for the porosity of the solid phase is the permeability of K. According to [12] the permeability is given by the empirical relation:

$$K = \kappa f_l^2$$

in which κ is taken as a constant and equal for all directions.

4. Deformation Model

In the following it is assumed, for simplicity, that the steel strand is cylindrical, although the actual product has a square cross section. Because of the axisymmetric cooling conditions imposed on the string, it is assumed that the entire solidification process has this same symmetry.

In the past, most of the effort has been devoted to solving the energy equation (Equation (7)) alone. This can easily be done if use is made of a few simplifications. First of all, because the steel bloom is much longer than it is thick, thermal conduction in the longitudinal direction (z-coordinate) can be neglected compared with thermal conduction in the radial (r-coordinate) direction. Secondly, it is assumed that deformations have a negligible effect on heat transport and that the steel moves with a constant speed (the casting speed u). Thirdly, it is assumed that macrosegregation doesn't influence the temperature distribution inside the bloom. It is then possible to use a microsegregation model (like the one proposed in [2] which is explained in more detail in the appendix) everywhere in the bloom, which provides an additional equation to link locally the volume fraction of solid, f_s, with the temperature T. This equation then, together with the energy equation itself, makes it possible to calculate the temperature distribution inside the bloom.

Such calculations have been described in, amongst others, [14] and in [5]. In the latter case, it was observed from these calculations that the temperature in the center of the product dropped, in the later stages of the solidification, much faster

than the temperature at the surface. The authors used this observation to construct a model that could, at least qualitatively, explain the observed macrosegregation pattern.

They assumed that, because of the small temperature drop of the surface of the product, the outer part of the cast product did not shrink much near the end of the solidification process. The inner part (with a much larger temperature drop) however, did shrink significantly. Since inner and outer part are connected, it was assumed that the inner part shrank towards the outer part, resulting in a volume expansion in the center of the steel strand near the end of the solidification process. This expansion was supposed to suck liquid steel to the center from its surroundings. Since the equilibrium distribution ration k_i is less than 1 for all dissolved elements, the liquid steel in the mushy zone will have a high concentration of these elements. The liquid sucked into the center will therefore enrich the center, thereby depleting its surroundings. In this way, qualitatively, the segregation pattern as shown in Figure 1 can be explained.

The model of the deformations that occur in the solidifying steel bloom is described in this section. In order to describe the deformations of the solid phase its velocity $\vec{v}_s$ is needed. This can be seen if it is realized that deformations occur because of a displacement of solid and that $\vec{v}_s$ is the displacement velocity of the solid. Since deformations are really displacements of some part of the solid relative to another part, the gradients of the velocity must be involved. It then turns out that $\nabla \cdot \vec{v}_s$ can be interpreted as the relative change of volume of a material (i.e. Lagrangian) volume element per time unit. Hence, if equations from which $\vec{v}_s$ can be calculated are specified then the deformations are known. A schematic model has been used in this study because of the different and complex processes taking place (thermal deformation of the solid shell and of the solid phase in the mushy zone; the ferrostatic pressure exerted by the liquid core; externally imposed deformations caused by the casting machine). First of all, it is assumed (based on the original idea in [5]) that the only deformations that are important are thermal deformations. Secondly, the complicated structure of the bloom was dealt with. Part of it is completely solid, part of it is completely liquid and part of it is a mixture of solid and liquid. To account for these different parts of the bloom, in line with [10], the bloom was divided into 4 zones, each of which deforms in its own special way (see Figure 2).

Zone I is the solid shell. It is bounded by the surface of the product and the solidus surface. Since the basic deformation is assumed to be a volume expansion in the center of the bloom, we neglect all deformations in zone I.

Zone II is bounded by the solidus surface and the surface for which $f_s = 0.1$. In this zone a solid structure is present. The solid skin in zone II contracts during the casting process and as explained earlier, only thermal contraction was taken into account. The governing equations are given by:

$$\nabla \cdot (\rho_s \vec{v}_s) = 0 \tag{9}$$

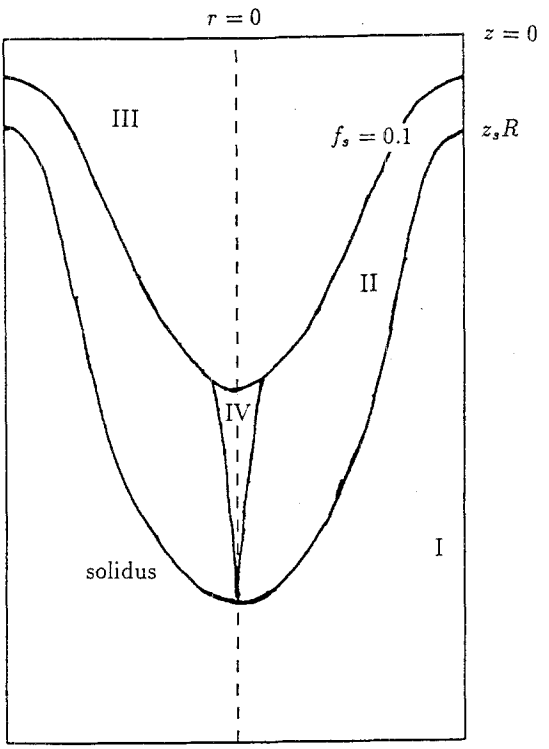

Fig. 2. Schematical representation of the different zones in the bloom, each of which deforms in its own way. z_{sR} denotes the z-position where the solidus line reaches the outer surface ($r = R$).

$$\rho_s(T) = \rho_s(T_0)\exp(-\alpha_s(T - T_0)) \tag{10}$$

in which T_0 denotes an arbitrary reference temperature and α_s the thermal expansion coefficient of steel.

Zone III is bounded by the fluid meniscus at the top of the steel bloom and by the surface for which $f_s = 0.1$. Although there is some solid material present in this zone, it is assumed that there is no solid *structure* and therefore there are no deformations in this zone.

Finally, zone IV consists of a small tubular piece of mushy material in the center of the bloom. In a cross section this is the hottest and consequently the weakest part of the bloom and therefore it is assumed that this zone deforms only as a reaction to deformations imposed by the surrounding zones. According to [8] the ratio between the diameters of zones IV and II is taken to be 0.1.

5. Computational Procedure

Having specified the deformation model, the equations (Equations (9) and (10)) that should permit the calculation of the velocity of the solid are now available.

Hence, the equations for calculating the temperature T (energy Equation (7)), the solute concentrations $\bar{c}_{si}$ (Equation (2)) and c_{li} (Equation (6)), the velocities $\vec{v}_l$ (the d'Arcy-equation (8)) and $\vec{v}_s$ (the deformation Equations (9) and (10)) and pressure p (total mass balance, Equation (1)) are available. In principle, all equations are coupled and must therefore be solved simultaneously. However, due to the complicated interactions between the different variables this would be a complicated thing to do and if numerical difficulties were to be encountered, it would be hard to find their cause. It is expected that the consequences of this decoupling are not very large, since it is a well-known fact that the temperature distribution can be satisfactorily calculated from the energy Equation (7) (with the help of a microsegregation model). Especially since the temperature is, in the present crude deformation model, the most important quantity, it is reasonable to expect this decoupling of the solving of the equations not to have a large effect. Hence, the following computational procedure was used for performing the calculations:

Step 1. Effects of deformations and macrosegregation are neglected. The temperature is calculated with the help of the energy Equation (7) and of the microsegregation model of [2]. Thermal conduction in the axial direction is neglected compared to thermal conduction in the radial direction (this is the type of calculation performed in [5] and [14]). In this way the temperature is obtained.

Boundary conditions: $z = 0\ T = T_{\text{cast}}\ c_{li} = c_{0i}$
$r = 0\ \partial T/\partial r = 0$
$r = R$ Either T or $\partial T/\partial r$ is specified.

In these conditions T_{cast} is the casting temperature and c_{0i} is the nominal concentration of solute i present in the steel.

Step 2. With the known temperature field, the deformations are calculated with the help of Equations (9) and (10). It has been assumed that the deformations are concentrated in the radial direction and that no deformation takes place in the axial direction. Hence v_{sz} is taken to be constant and equal to the casting speed u. This calculation then provides us with the velocity of the solid phase. Boundary conditions: at solidus isotherm $v_{sr} = 0$.

Step 3. The volume fraction f_s is calculated from the energy equation (Equation (7)). To be able to do this, it is assumed that deformations have a negligible effect on the temperature field and that they only influence the f_s-values. Using this assumption, the energy equation can be considered to be an equation in which only the f_s-values are unknown. Hence, the energy equation becomes a differential equation from which the f_s-values can be calculated.

Boundary conditions: $z = 0\ f_s = 0$
$r = 0\ \partial f_s / \partial r = 0$

Step 4. With the help of the now known f_s and $\vec{v}_s$-values, it is possible to calculate the liquid velocity $\vec{v}_l$ using the equations for the mass balance (Equation (1)) and the d'Arcy-equation 8. Although the d'Arcy-equation, strictly speaking, only holds for the mushy zone, it has been used also in the region where there's only fluid. This can be done by setting $f_l = 1$ in the d'Arcy-equation. The effect of this step is that in this region a uniform velocity profile exists, where a Poiseuille-profile would be expected.

Boundary conditions: $r = 0\ v_{lr} = 0$
$r = R$ and $z < z_{sR}\ v_{lr} = 0$
$z = 0\ v_{lz} = (\rho_s / \rho_l) u$ and $v_{lr} = 0$.

Step 5. Finally, the Equations (2) and (6) for the solute mass are solved to obtain c_{li} and $\bar{c}_{si}$ and hence the concentration distribution is obtained.

Boundary conditions: $z = 0\ c_{li} = c_{0i}$
$r = 0\ \partial c_{li} / \partial r = 0$
$r = 0\ \partial \bar{c}_{si} / \partial r = 0$

6. Results

As a test situation calculations for a high carbon steel grade, impured with a small amount of phosphor were performed. The actual cooling conditions imposed, were taken from measurements performed at Hoogovens IJmuiden. The values of the constants that occur in the governing differential equations and in the boundary conditions are tabulated in Table I.

The values of the permeability constant κ and the liquid viscosity μ are not specified. The reason for this is the fact that they only occur as the ratio (κ/μ) in the d'Arcy-equation. It can be proven that the value of the ratio κ/μ only determines the magnitude of the pressure gradient $\vec{\nabla} p$ but that its value has *no* influence on the actual distribution of $\vec{v}_l$ which is what we're interested in. Hence, the values of κ and μ do not influence the final concentration distribution.

Results are presented in Figures 3 and 4. Figure 3 shows the development of $\bar{c}_{si}/c_{0i}$ (in which c_{0i} denotes the nominal concentration of solute i in the steel) as a function of the volume fraction f_s at the centerline of the steel ($r = 0$) for both carbon and phosphor. Noteworthy are the sharp transitions in the $\bar{c}_{si}/c_{0i}$-curves near $f_s = 0$ (for both carbon and phosphor) and near $f_s = 1$ (for phosphor only). The principal reason for the sharp transition near $f_s = 0$ and the resulting discontinuity, is the fact that for $f_s = 0$, there is no solid phase present and hence, the value of $\bar{c}_{si}$ is undefined. In the numerical implementation this value has been taken equal

TABLE I. Values used in calculations

Constant	Value	Unit
$c_{0(\text{carbon})}$	1	%
$c_{0(\text{phosphor})}$	0.01	%
c_p	670	J/kgK
$\vec{g}$	9.81	m/s^2
k_{carbon}	0.35	–
k_{phosphor}	0.06	–
L	2.72×10^5	J/kg
R	0.05	m
T_{cast}	1833	K
u	0.05	m/s
α_s	8×10^{-5}	–
γ_{carbon}	1	–
γ_{phosphor}	0.01	–
λ	30.0	W/mK
ρ_l	7.0×10^3	kg/m^3
ρ_s	7.4×10^3	kg/m^3

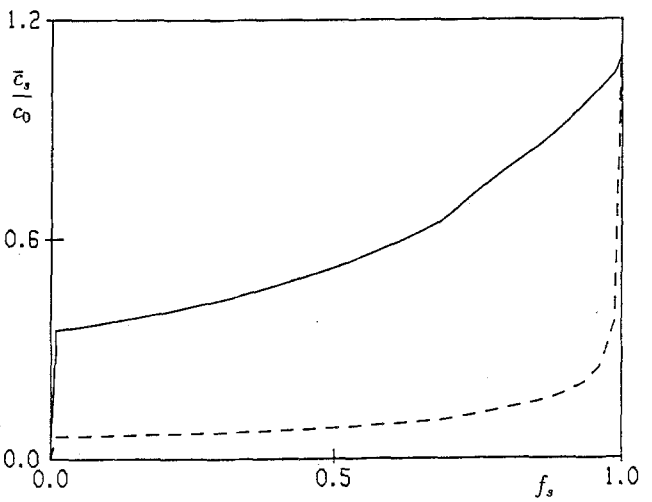

Fig. 3. Development of the carbon concentration as a function of the solid volume fraction in the center of the product for both carbon and phosphor. —— carbon; - - - - - - phosphor.

to 0 (numerically speaking the actual value taken for $\bar{c}_{si}$ in the liquid region is irrelevant since it is multiplied in the transport equation with f_s which is 0 in the liquid region). However, the first solid formed will have $\bar{c}_{si} = k_i c_{li} \approx k_i c_{0i}$ and thus, $\bar{c}_{si}/c_{0i} \approx k_i$. Hence, in the first numerical volume-element which has $f_s > 0$, there is a sharp transition in the $\bar{c}_{si}/c_{0i}$-graph. Hence, the discontinuities. Similar

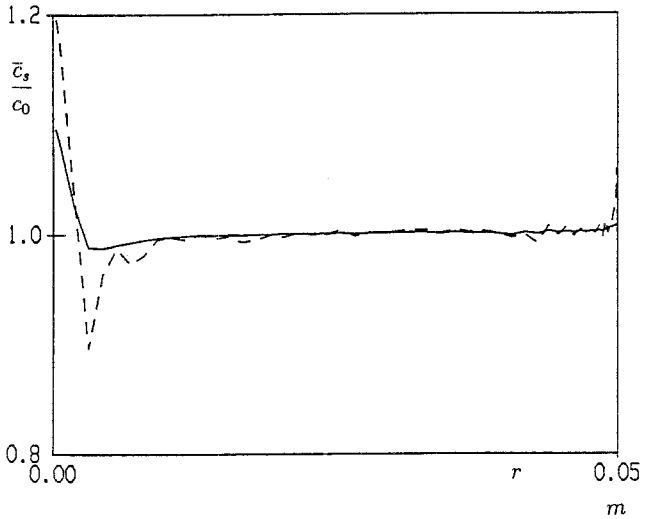

Fig. 4. Distribution of the calculated concentrations in the bloom after solidification as a function of the distance to the center of the product. —— carbon; - - - - - - phosphor.

results were obtained, using microsegregation models (see [4]). Hence, these sharp transitions do not seem to matter very much in our numerical procedure.

The most interesting result is depicted in Figure 4. This figure shows the *radial* distribution of $\bar{c}_{si}/c_{0i}$, in which the interest lies. As can be seen, the calculations show the characteristics as found in measurements (Figure 1): there's a large peak of positive segregation in the center of the bloom ($r = 0$) with a slight negative segregation at its side and with a more or less constant concentration distribution (with a concentration approximately equal to the nominal concentration) in the rest of the steel. The values calculated for $\bar{c}_{si}/c_{0i}$ at the center are approximately 1.1 for carbon and 1.2 for phosphor. These values agree well with the measured values in spite of the relatively crude model that was used to calculate the centerline macrosegregation.

7. Conclusions

Although this study is of a preliminary nature, it can be concluded that the model used in this study, captured the important effects of centerline macrosegregation. This was possible, in spite of all the simplifications made in the model and in the computational procedure. Hence, it can be concluded that thermal deformations in the mushy zone are the main cause of centerline macrosegregation and that it is essential to capture these deformations well as our model seems to do. Another important conclusion that can be drawn is the fact that it has been possible to perform *all* calculations (including those describing the deformations in the mushy zone) within a general Computational Fluid Dynamics code (PHOENICS). This

means that time can be saved programming the equations and that *general* software (as incorporated in PHOENICS) can be used to solve the problem.

Appendix

In section 3 it was mentioned that the parameter γ_i, which is a measure of the diffusion of solute i in the solid phase, could be linked to several parameters that occur in the microsegregation model originally proposed in [2]. In this model, a solute mass balance is taken over a secundary dendrite arm and (with several assumptions) this then leads to an equation giving a relation between the concentration of solute c_{li} and the volume fraction f_s. If the correction, proposed in [3] is taken into account in the original model of [2], the equation describing c_{li} as a function of f_s reads:

$$c_{li} = c_{0i}(1 - (1 - 2\bar{\alpha}_i k_i) f_s)^{\frac{k_i - 1}{1 - 2\bar{\alpha}_i k_i}} \tag{11}$$

in which $\bar{\alpha}_i$ is given by the relations:

$$\begin{aligned} \bar{\alpha}_i &= \alpha_i \left(1 - \exp\left(-\frac{1}{\alpha_i}\right)\right) - \frac{1}{2}\exp\left(-\frac{1}{2\alpha_i}\right) \\ \alpha_i &= 4\frac{D_{si} t_s}{L_d^2}. \end{aligned}$$

The parameters D_{si}, t_s and L_d denote respectively the molecular diffusion coefficient of solute i in the solid, the solidification time and the secundary dendrite arm spacing. These parameters can be either measured or calculated ([4]) and this provides the means of calculating $\bar{\alpha}_i$.

An alternative method of determining Equation (11) using the equations derived in section 3 of this article is presented here. Take as a starting point Equation (6) for the solute concentration in the liquid:

$$\nabla \cdot (\rho_l f_l \vec{v}_l c_{li}) = (\gamma_i - 1) k_i c_{li} \nabla \cdot (\rho_s f_s \vec{v}_s) - \gamma_i \nabla \cdot (\rho_s f_s k_i \vec{v}_s c_{li}).$$

It is assumed that there is no macrosegregation and no deformation of the solid. These assumptions are expressed by the relations:

$$\begin{aligned} \rho_s &= \rho_l = \rho \quad \text{and} \quad \rho \quad \text{constant} \\ v_{lr} &= v_{sr} = 0 \\ v_{lz} &= v_{sz} = u \end{aligned}$$

in which u denotes the casting speed.

Substitution of these expressions in Equation (6) gives:

$$((1 - f_s) + \gamma_i k_i f_s)\frac{\mathrm{d}c_{li}}{\mathrm{d}z} = (1 - k_i) c_{li} \frac{\mathrm{d}f_s}{\mathrm{d}z}.$$

Integration of this equation with the boundary condition $c_{li}(f_s = 0) = c_{0i}$ gives:

$$c_{li} = c_{0i}(1 - (1 - \gamma_i k_i) f_s)^{\frac{k_i - 1}{1 - \gamma_i k_i}}.$$

This equation now has the same form as Equation (11). Hence, it can be concluded that the parameter γ_i is given by the relation:

$$\gamma_i = 2\bar{\alpha}_i. \tag{12}$$

The importance of this result is that it provides the means of estimating the parameter in a well known microsegregation model and hence, the possibility of giving a quantitatave estimate of the parameter's value for the different elements.

References

1. Bear, J. and Yavuz Corapcioglu, M., *Fundamentals of transport phenomena in porous media.* NATO Advanced Studies. Dordrecht: Martinus Nijhoff Publishers (1982).
2. Brody, H. D. and Flemings, M. C., *Trans. Met. Soc. AIME.* 236 (1966) 615–623.
3. Clyne, T. W. and Kurz, W., *Metall. Trans.* 12A (1981) 965–971.
4. Cornelissen, M. C. M., Mathematical model for the solidification of multicomponent alloys. *Iron and steelmaking* 13 (4) (1986) 204–212.
5. Engström, G., Frederiksson, H. and Rogberg, B., On the mechanisms of macrosegregation formation in continuous cast steels. *Scand. J. Metall.* 12 (1983) 3–12.
6. Flemings, M. C. and Nereo, G. E., Macrosegregation: part I. *Trans. Met. Soc. AIME* 239 (1967) 1449–1461.
7. Fuji, T., Poirier, D. R. and Flemings, M. C., Macrosegregation in a multicomponent low alloy steel. *Metall. Trans.* 12B (1979) 331–339.
8. Lesoult, G., Étude comparative des differentes composantes du mouvement du métal liquide dans la zône pâteuse au cours de la solidification des alliages á l'aide d'un bilan de masse local. *C. R. Acad. Sc. Paris* 304 série II no. 16 (1987) 977–980.
9. Lesoult, G., Ruer, J., Gilquin, P. and Sella, S., Influence of heat transfer, mechanical behaviour of the mushy zone and electromagnetic stirring on the segregations in C. C. billets and blooms. *Continuous Casting 88* Brussels (1988).
10. Lesoult, G. and Sella, S., Spongy behaviour of alloys during solidification. In: G. Martin and L. P. Kubin (eds), *Nonlinear Phenomena in Materials Science.* Trans. Tech Publications (1988).
11. Mehrabian, R., Keane, M. and Flemings, M. C., Interdendritic fluid flow and macrosegregation; influence of gravity. *Metall. Trans.* 1 (1970) 1209–1220.
12. Miyazawa, K. and Schwerdtfeger, K., Macrosegregation in continuously cast steel slabs: preliminary theoretical investigation on the effect of steady state bulging. *Archiv. Eisenhüttenwes.* 52 (1981) 415–422.
13. Rosten, H. I. and Spalding, D. B., The PHOENICS beginner's guide. Surrey: Beechgrove Press (1987).
14. Ruer, J., Sella, S. and Dulac, P.-Y., A numerical approach of the segregation phenomenon and electromagnetic stirring in continuous casting.
15. Tacke, K., Grill, G., Miyazawa, K. and Schwerdtfeger, K., Macrosegregation in strand cast steel: computation of concentration profiles with a diffusion model. *Archiv. Eisenhüttenwes.* 52 (1981) 15–20.